Detection of Abnormal Diffuse Perfusion in SPECT Using a Normal Brain Atlas

Jean-François Laliberté[a], Jean Meunier[a], Max Mignotte[a], and Jean-Paul Soucy[b]

[a] DIRO, Département d'Informatique et de Recherche Opérationnelle, University of Montréal
P.O. 6128, succ. Centre-ville, Montréal, Canada (Québec), H3C3J7.
[b] CHUM (University Hospital), University of Montréal,
1560 Sherbrooke Street East, Montréal, Canada, H2L 4M1

ABSTRACT

Despite the advent of sophisticated image analysis algorithms, most SPECT (Single Photon Emission Computerized Tomography) cerebral perfusion studies are assessed visually, leading to unavoidable and significant inter and intra-observer variability. Here, we present an automatic method for evaluating SPECT studies based on a computerized atlas of normal regional cerebral blood flow (rCBF). To generate the atlas, normal (screened volunteers) brain SPECT studies are registered with an affine transformation to one of them arbitrarily selected as reference to remove any size and orientation variations that are assumed irrelevant for our analysis. Then a smooth non-linear registration is performed to reveal the local activity pattern displacement among the normal subjects. By computing and applying the mean displacement to the reference SPECT image, one obtain the atlas that is the normal mean distribution of the rCBF (up to an affine transformation difference). To complete the atlas we add the intensity variance with the displacement mean and variance of the activity pattern. To investigate a patient's condition, we proceed similarly to the atlas construction phase. We first register the patient's SPECT volume to the atlas with an affine transformation. Then the algorithm computes the non-linear 3D displacement of each voxel needed for an almost perfect shape (but not intensity) fit with the atlas. For each brain voxel, if the intensity difference between the atlas and the registered patient is higher than normal differences then this voxel is counted as "abnormal" and similarly if the 3D motion necessary to move the voxel to its registered position is not within the normal displacements. Our hypothesis is that this number of abnormal voxels discriminates between normal and abnormal studies. A Markovian segmentation algorithm that we have presented elsewhere is also used to identify the white and gray matters for regional analysis. We validated this approach using 23 SPECT perfusion studies (^{99m}Tc ECD) selected visually for clear diffuse anomalies (a much more stringent test than "easy" focal lesions detection) and 21 normal studies. A leave-one-out strategy was used to test our approach to avoid any bias. Based on the number of "abnormal" voxels, two simple supervised classifiers were tested: (1) minimum distance-to-mean and (2) Bayesian. A voxel was considered "abnormal" if its P value with respect to the atlas was lower that 0.01 (1%). The results show that for the whole brain, a combination of the number of intensity and displacement "abnormal" voxel is a powerful discriminant with a 91% classification rate. If we focus only on the voxels in the segmented gray matter the rates are slighty higher.

Keywords: SPECT, brain, atlas, classification, optical flow, segmentation, Markov

1. INTRODUCTION

The close coupling generally observed between local cerebral metabolic activity, reflecting mostly synaptic activity, and regional cerebral blood flow (rCBF), make the study of the later a potential approach to that of the former. This became particularly interesting in the mid 1980's with the advent of widespread availability of clinically applicable cerebral perfusion studies, based on the intravenous injection of Technetium-99m labeled tracers (e.g. ^{99m}Tc HMPAO or ^{99m}Tc ECD) which show a cerebral distribution reasonably well correlated with that of perfusion.[1] This distribution is then assessed with Single Photon Emission Computed Tomography (SPECT), which generates a three dimensional image of the distribution of activity, which is then assimilated

to the distribution of cerebral blood flow. This technique has made it possible for all clinical nuclear medicine department to perform rCBF studies which were previously limited to a few centers with access to highly specialized SPECT ^{133}Xe dynamic scanners, Positron Emission Tomography (PET) or functional Magnetic Resonance Imaging (fMRI).

Despite the advent of sophisticated image analysis algorithms, most clinical assessments of the normality, or deviation from it, of the distribution of rCBF in SPECT, are currently done by visual observation of the studies, searching for side-to-side asymmetries or other "abnormalities" (highly subjective evaluations of the "homogeneity" of distribution, etc.) as referred to what could be observed in normal cases. In fact, most centers did not even use a true normal bank of data, but rather a more or less informed hypothetical mental construct of what normal studies should look like.

Different methods have been described to compare accurately the acquired volume of data within a reference one, thereby ensuring identification of regions with modified accumulation of the rCBF tracer. This implies more or less sophisticated registration algorithms. Once positioning is performed, numerous techniques have been developed to analyze, based on predefined "statistical" criteria, variations in the distribution of activity of the brain between patients and normal or from one study condition to another. For example, SPM, a very nice and powerful package is offered to the scientific community by the Methodology Group at the Wellcome Department of Cognitive Neurology, UK, under the supervision of Karl Friston[2,3] . SPM stands for Statistical Parametric Mapping.

Most of the work in this field has been applied to PET and fMRI studies at this time, but several problems are essentially the same in SPECT, and the principles applied to one type of imaging can often be applied to the other. However, applications in SPECT remain scarce and are not generally available to clinicians, moreover, no consensus exists as to the optimal techniques to be employed.

In this paper, we present and test a method for evaluating SPECT studies based on a computerized atlas of normal regional cerebral blood flow (rCBF). The methodology stems from our previous work on anatomical atlas construction.[4] In that work we have described a completely automatic procedure to build a "stable" average anatomical model of the human brain using a set of magnetic resonance (MR) images. This model or atlas contains two important features: an average intensity (with the its normal variations for each voxel) and an average shape (with the normal shape deformation as a x, y, z covariance matrix for each voxel). In SPECT imaging the atlas will contain for each voxel, both the normal rCBF (mean intensity and variance) and the extent of possible displacement of the activity pattern (as the displacement magnitude mean and variance).

2. METHOD

Two main steps are needed in our strategy to detect abnormal diffuse perfusion in SPECT. The first step is the construction of an atlas of the normal brain in SPECT and the second step is to classify a patient as normal or abnormal by comparing his SPECT study with the atlas. An additional step that could be useful is presented to isolate a particular region of interest in the brain such as the gray matter.

2.1. Atlas construction

The atlas construction involves several normal SPECT studies that must be gathered into a unique reference volume. For this purpose we must first normalize the intensity to take into account different acquisition parameters. Then the SPECT volumes must be registered using a linear transformation to make all brains comparable in size and orientation. Finally the third step computes the individual SPECT pattern shape differences that will be incorporated in the atlas with the mean intensity and variance. These atlas construction steps are described below.

2.1.1. Intensity normalization

The registration algorithm assumes the same intensity for corresponding brain structures in the two images to be aligned. For miscellaneous reasons, such as acquisition parameters or pre- and post-processing, this may not be the case. To rectify these intensity differences, a linear correction is evaluated. Assuming an initial rough registration of the two brain images, a joint histogram is computed. The slope of a linear regression through

this histogram gives the multiplication factor to compensate for the overall intensity difference. If necessary this evaluation can be done iteratively during the registration procedure to improve its accuracy.
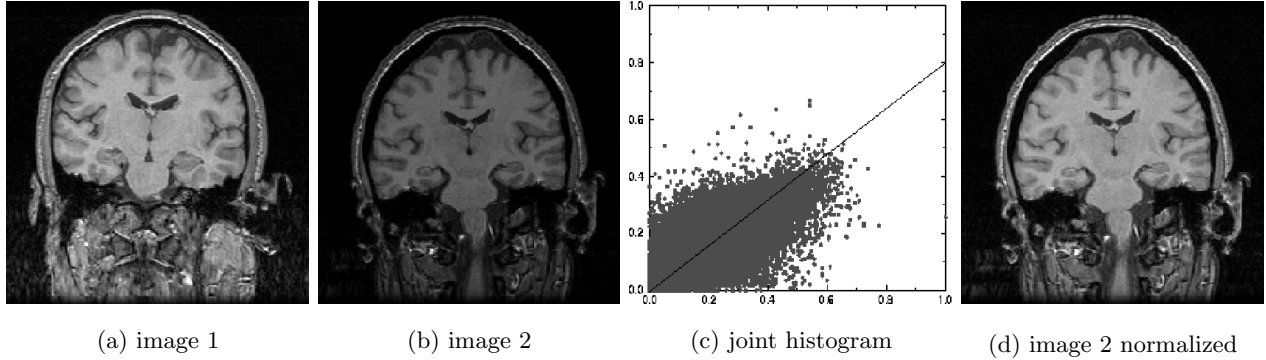

(a) image 1   (b) image 2   (c) joint histogram   (d) image 2 normalized

Figure 1. Image Normalization in MRI, adapted from[4]

2.1.2. Linear registration

A 3D image sequence (of two or more images) can be mathematically described as a function $I(x, y, z, t)$ where I is the image intensity at time t and position (x, y, z). Using the chain rule for derivatives, one obtains the basic constraint of optical flow.[5]

$$\frac{dI}{dt} = \frac{\partial I}{\partial x}\frac{dx}{dt} + \frac{\partial I}{\partial y}\frac{dy}{dt} + \frac{\partial I}{\partial z}\frac{dz}{dt} + \frac{\partial I}{\partial t} \tag{1}$$

The partial derivatives can be estimated directly from two SPECT images to be registered. The four remaining variables dx/dt, dy/dt, dz/dt and dI/dt represent respectively the motion (velocity) along the x, y and z axes and the object (brain) brightness changes. This equation lays down a first constraint to determine the motion (registration) between two SPECT images. The linearity condition provides another constraint:

$$\begin{bmatrix} \frac{dx}{dt} \\ \frac{dy}{dt} \\ \frac{dz}{dt} \end{bmatrix} = \overrightarrow{T} + M \begin{bmatrix} x \\ y \\ z \end{bmatrix} \tag{2}$$

where $\overrightarrow{T}$ and M are translation vector and 3×3 matrix respectively. A last constraint is used to model the behavior of the brightness changes dI/dt. One usual option is to set dI/dt to 0, which means no change in object (brain) intensities.[5] Overall, this constraint is correct when the brain SPECT images are first intensity normalized as described in the previous section.

The overdetermined system obtained by writing down the basic optical flow equation using the linearity and dI/dt constraints for each voxel, can be solved using a least square fit. In this way, one obtains the linear field transformation needed to align both brain SPECT volumes and to give them the same size and orientation. If necessary this approach can be used iteratively by keeping track of intermediate results[6,7] to improve the results when the two brains are far from being aligned in the original images.

2.1.3. Non-linear registration

To compute the non-linear residual transformation to better register both volumes, we adapt the Horn and Schunk algorithm.[5] The algorithm initially computes the x, y and z motions $U = dx/dt$, $V = dy/dt$ and $W = dz/dt$ using the optical flow brightness constraint (eq. 1) to get an initial solution (motion component perpendicular to the gray-level isocontours):

$$U = -\frac{\partial I}{\partial x}\frac{\frac{\partial I}{\partial t}}{||\nabla I||^2 + \alpha^2} \qquad V = -\frac{\partial I}{\partial y}\frac{\frac{\partial I}{\partial t}}{||\nabla I||^2 + \alpha^2} \qquad W = -\frac{\partial I}{\partial z}\frac{\frac{\partial I}{\partial t}}{||\nabla I||^2 + \alpha^2} \qquad (3)$$

then iteratively the optical flow (U, V, W) is smoothed (local average) and at that point updated to the nearest solution of the brightness constraint equation:

$$U^{k+1} = \overline{U}^k - \frac{\partial I}{\partial x}\frac{\nabla I \cdot (\overline{U}^k, \overline{V}^k, \overline{W}^k) + \frac{\partial I}{\partial t}}{||\nabla I||^2 + \alpha^2}$$

$$V^{k+1} = \overline{V}^k - \frac{\partial I}{\partial y}\frac{\nabla I \cdot (\overline{U}^k, \overline{V}^k, \overline{W}^k) + \frac{\partial I}{\partial t}}{||\nabla I||^2 + \alpha^2} \qquad (4)$$

$$W^{k+1} = \overline{W}^k - \frac{\partial I}{\partial z}\frac{\nabla I \cdot (\overline{U}^k, \overline{V}^k, \overline{W}^k) + \frac{\partial I}{\partial t}}{||\nabla I||^2 + \alpha^2}$$

where the bar over $\overline{U}^k$ represent local average (using a $3 \times 3 \times 3$ mean filter) at the kth iteration. The α^2 term is used to avoid unreliable results introduced by low value $||\nabla I||$ and also to give precedence of high value $||\nabla I||$ in the iterative process; this means that high contrast contours will drive the non-linear warping, otherwise any small inter-patient brightness changes would affect (inaccurately) the warping process. In this study, we found after several tests that $\alpha = 100$ was a good choice to insure good separability of the normal and abnormal classes (see below). The resulting non-linear field is smooth and allows a better registration of both SPECT volume; however it cannot be use without a prior linear registration otherwise the spatial and temporal derivatives risk to become unreliable.

2.1.4. Atlas Construction Principles

After linear volume registration and intensity correction of all normal brains to be incorporated into the atlas, its construction can begin as illustrated in the figure 2 scheme.
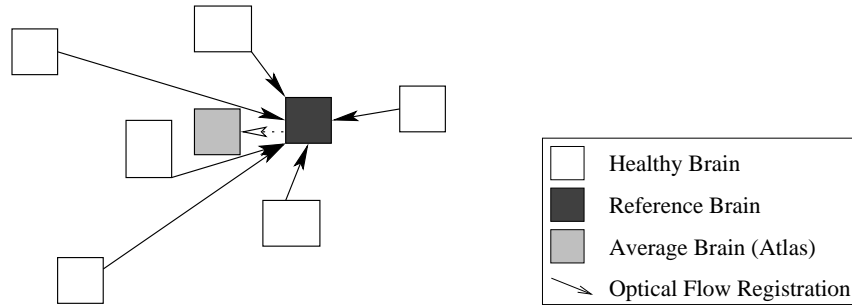

Figure 2. Atlas Construction

We start by selecting a brain in the group of normal brains as a reference (black square in fig. 2). Then we register the rest of normal brains (white squares) on this reference one with the non-linear optical flow procedure described in the previous section. Then the mean intensity and its variance can be computed. However since the reference brain has not necessarily the (true) average brain shape, the mean displacement of all the normal brains is calculated and subtracted from the reference brain to obtain the average brain shape and intensity (gray square). The final atlas consists of this average with the intensity variance as well as the normal local displacement (variance of the displacement magnitude) of the activity pattern.

2.2. Classification

To investigate a patient condition, we proceed similarly to the atlas construction phase. We first register the patient's SPECT volume to the atlas (average brain intensity and shape) with an affine transformation with the procedure described in section 2.1.2. Then the algorithm computes the non-linear 3D displacement of each voxel needed for an almost perfect shape (but not intensity) fit with the atlas (section 2.1.3). For each patient's brain voxel we are then able to compare the intensity and non-linear displacement with their normal values in the reference system of the atlas. However this represents a huge amount of data (attributes) for any classification algorithm. To reduce the dimensionality of the problem, we use the following procedure.

For each brain voxel, if the intensity difference between the atlas and the registered patient is higher than normal differences than this voxel is counted as "abnormal" and similarly if the 3D motion amplitude necessary to move the voxel to its registered position is not within the normal displacements. Our hypothesis is that this number of abnormal voxels discriminates between normal and abnormal studies. Assuming a Gaussian probability density function (*pdf*) for the intensity and motion attributes, if the voxel attribute value probability is less than 1%, this pixel is considered an outlier (abnormal).

With the reduction of dimensionality, we now consider only the number of outliers for intensity and the number of outliers for displacement as the two new attributes for classification. Obviously we expect normal individuals to show relatively small numbers of outliers while the reverse is true for patients suffering from brain diffuse perfusion disorders. To classify between normal and abnormal brain we tested two very simple classifiers. The first one is the minimal distance classifier where one simply counts the number of outliers and choose the class with the nearest mean number of outliers. Another slightly more complex classifier, the Bayes classifier, was tested and assigns the most likely class assuming a Gaussian *pdf* model for each class.

2.3. Region of interest (ROI) segmentation

The computation of brain voxel attributes requires first to identify the brain itself. In SPECT imaging this can generally be done quite easily by choosing a threshold of say 30% of the maximum number of counts (or gray level) sometimes with some more processing. However one could be interested in investigating the attributes in a particular region of interest (ROI) of the brain. For instance, since we are considering abnormal diffuse perfusions that typically occur in the gray matter, we believe that its identification could be useful. A threshold approach will not be efficient here because too much voxels in the gray matter share the same gray levels as the white matter. To solve this problem we use a Markovian segmentation algorithm that we have presented elsewhere[8,9] that will both identify the whole brain and its gray matter.

Markovian segmentation is quite complex because the estimation of *pdf* model parameters for each ROI is required before the segmentation could take place while this segmentation is necessary to estimate the parameters. This is clearly a chicken and egg problem. One way to solve this problem is to manually identify region of voxels in each region for parameter assessment but this would add an important burden to the clinician and could lead to inter- and intra- observer variability.

To overcome this problem we proposed a two step process. First, an automatic parameter estimation step in which we estimate the parameters of the gray level statistical distribution associated to each ROI in the SPECT volume. Here we assume that the CSF (CerebroSpinal Fluid) and background activities follow the same exponential probability distribution law in order to take into account the Poisson noise inherent to SPECT imaging. As for the gray values in the white and gray matters, they are modelled with two different Gaussian distributions. To fit those distributions to the data histogram, we use the ICE (Iterative Conditional Estimation) algorithm[8,9]. An estimation example is illustrated in figure 3 and table 1.

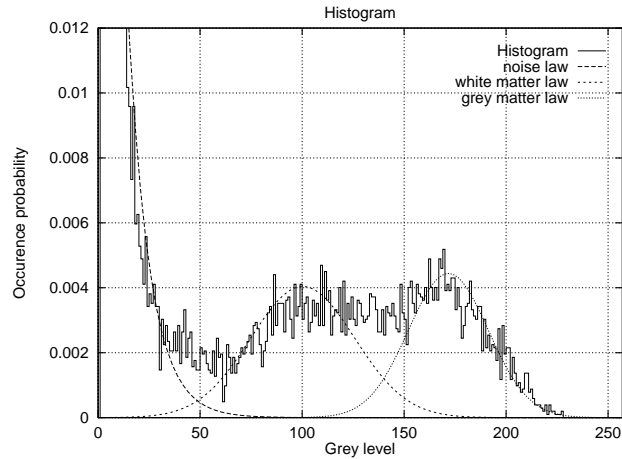|	π	μ	σ^2
CSF	0.52	11	—
White matter	0.26	100	648
Grey matter	0.22	172	283

Table 1. Intensity Estimation Values.

Figure 3. Intensity Estimation Histogram.

Second, the 3D Markovian segmentation itself is formulated as an optimization problem in a Bayesian framework through the use of the previous step parameters and an isotropic homogeneous Potts model with first order neighborhood to account for the spatial dependencies between voxels. In equation 5, the first term of the equation to be minimized involves the estimated distribution laws $P(y_s|x_s)$ previously computed and the second terms the Potts model for local homogeneity between the current voxel and its six neighbors. Segmentation results are presented in figure 4 as well as the original SPECT slices[8,9] .

$$\arg \min_x \sum_{s \in S} - \ln P_{Y_s|X_s}(y_s|x_s) + \sum_{<s,t>} (1 - \delta(x_s, x_t)) \tag{5}$$
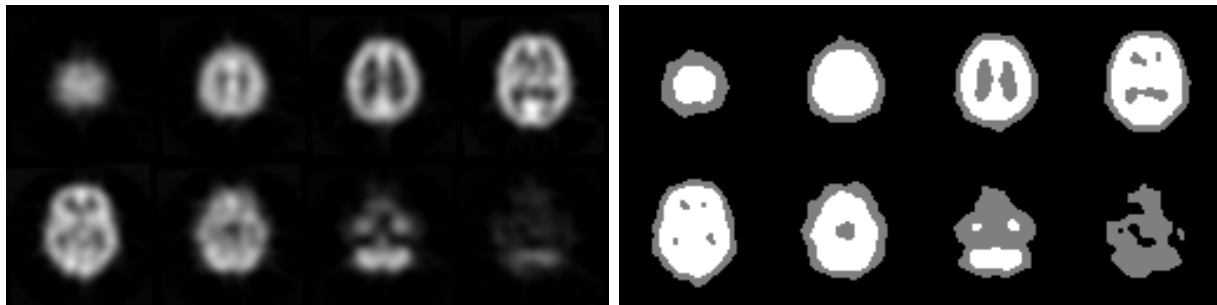
(a) original image

(b) segmented image

Figure 4. Brain Segmentation

3. RESULTS

3.1. Data sets

We validated this approach using 23 SPECT perfusion studies (^{99m}Tc ECD) selected visually for clear diffuse anomalies. The detection of abnormal diffuse perfusion is typically a difficult task and is certainly much more challenging than "easy" focal lesions detection for instance. The atlas was constructed with 21 perfusion

studies from normal volunteers (residents and physicians). Care was taken to keep as much as possible the same acquisition protocol (e.g. sampling, levels of statistics (counts), filtering, reconstruction and restoration methodologies) for all studies. Each transversal slice is 64 x 64 pixels and there are typically around 40 slices per individual. The number of count is rescaled for 8 bits pixels, that is 256 gray levels. The volume was padded with additional slices to get a set of uniform dimension volumes, that is $64 \times 64 \times 64$ voxels. The size of one voxel is $4.2 \times 4.2 \times 4.2$ millimiters.

3.2. Atlas construction

Figure 5 show the behavior of the registration process necessary for the atlas construction with image differences and mosaics. In figure 5.a, the difference between corresponding transaxial slices of two different brains shows clearly the misalignment (black, gray and white corresponding respectively to negative, no, and positive differences). After linear normalization for brain size and orientation (figure5.c), the difference falls considerably but not completely. This was expected since some groups[10,11], have shown in MRI that linear models will leave a residual RMS mis-match of 6-7 mm. Finally, figure 5.e presents the typical intensity differences that will be kept in the atlas after non-linear registration. Figures 5.b 5.d 5.f display the same results as mosaics where 8 x 64 pixels strips of each image appear in turn to help assess the registration process.

Figure 6 exhibits the SPECT rCBF normal atlas with gray level images. It consists in four kinds of information: (a) the intensity average, (b) the displacement magnitude average (c) the intensity variance (magnified for display purposes) and (d) the displacement variance (also normalized to 256 gray levels).

3.3. Validation

Due to the small data set, a leave-one-out strategy was used to test our approach in order to avoid any bias (fig 7). Essentially this means that in turn, one perfusion study is used to test the algorithm while the other ones are used for the atlas construction and classifier parameter estimation.

Table 2 shows the success rates for both classifiers using the number of intensity outliers, the number of displacement outliers, and both attributes for classification. As expected the more sophisticated algorithm (Bayes) gives the best results and in that case the use of both attributes is better.

	Minimal Distance Classifier	Bayes Classifier
Intensity	66.6%	88.8%
Pattern Displacement	80.0%	86.6%
Both	77.7%	91.1%

Table 2. Whole brain classification results.

Since we are considering abnormal diffuse perfusion that typically occurs in the gray matter, table 3 displays the success rates when only this ROI is considered. Again the Bayes classifier shows better results although the use of both attributes does not improve the success rate.

	Minimal Distance Classifier	Bayes Classifier
Intensity	73.3%	86.6%
Pattern Displacement	82.2%	93.3%
Both	88.8%	91.1%

Table 3. Gray matter only classification results.

(a) Image difference, no registration

(b) Image mosaic, no registration

(c) Image difference, affine registration

(d) Image mosaic, affine registration

(e) Image difference, non-linear registration

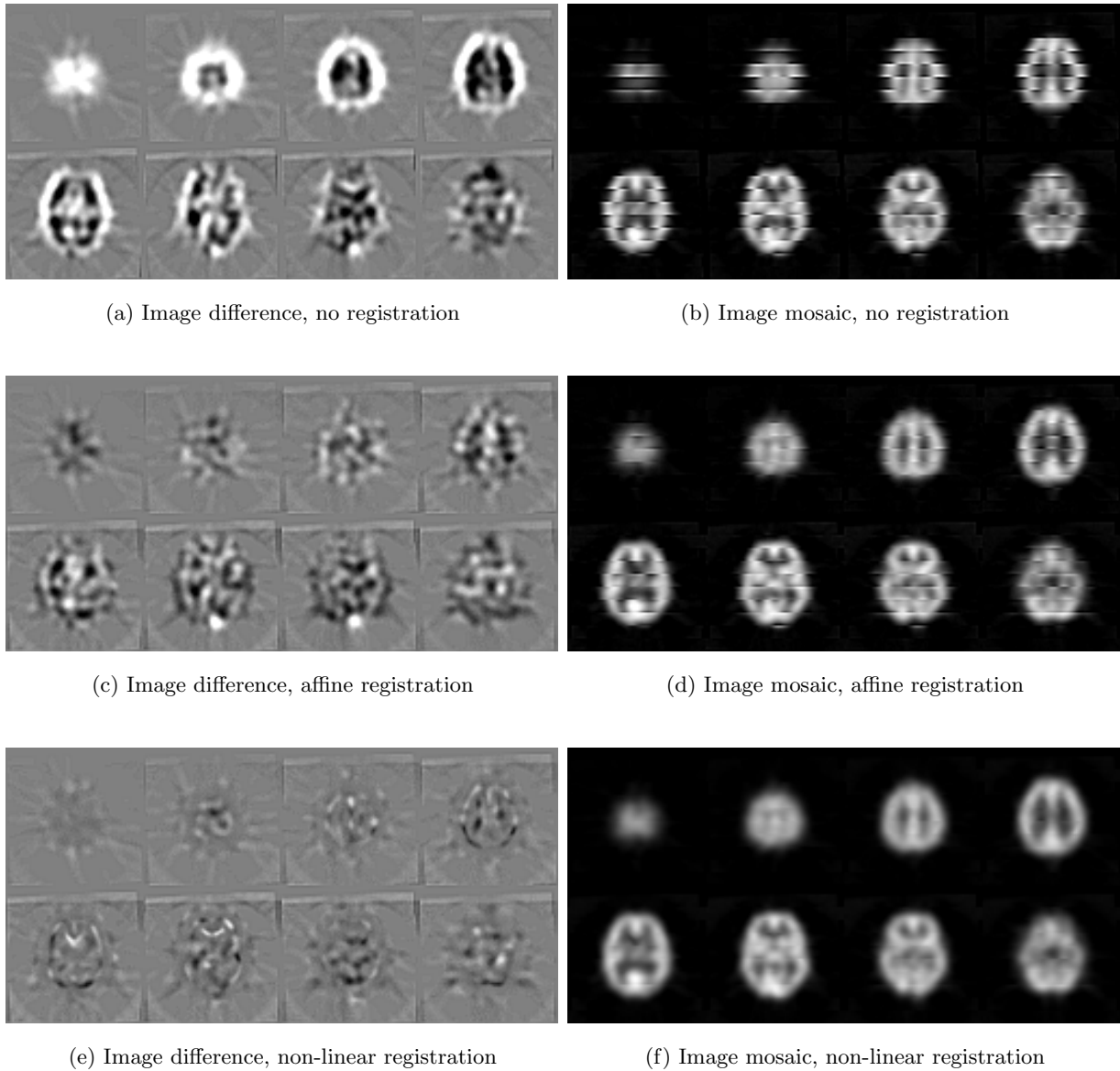(f) Image mosaic, non-linear registration

Figure 5. Registration process behavior

4. CONCLUSION

We have presented a method to successfully detect diffuse anomalies in SPECT imaging by using a normal rCBF numerical atlas containing for each voxel, both the normal rCBF (mean intensity and variance) and the extent of possible displacement of the activity pattern (as a displacement mean and variance). The reader can appreciate in figure 6 the low noise, relatively high contrast (for nuclear medicine images) and high visual quality of the mean intensity of the atlas.

We have then tested this atlas for detection of diffuse rCBF disorders with simple classification algorithms after dimensionality reduction. To our knowledge there is no other simple and automatic method to carry such a complex interpretation task (detection of diffuse anomalies in SPECT) with a success rate higher than 91% as obtained in this work. Thus, we believe that this methodology could greatly reduce the burden of assessing
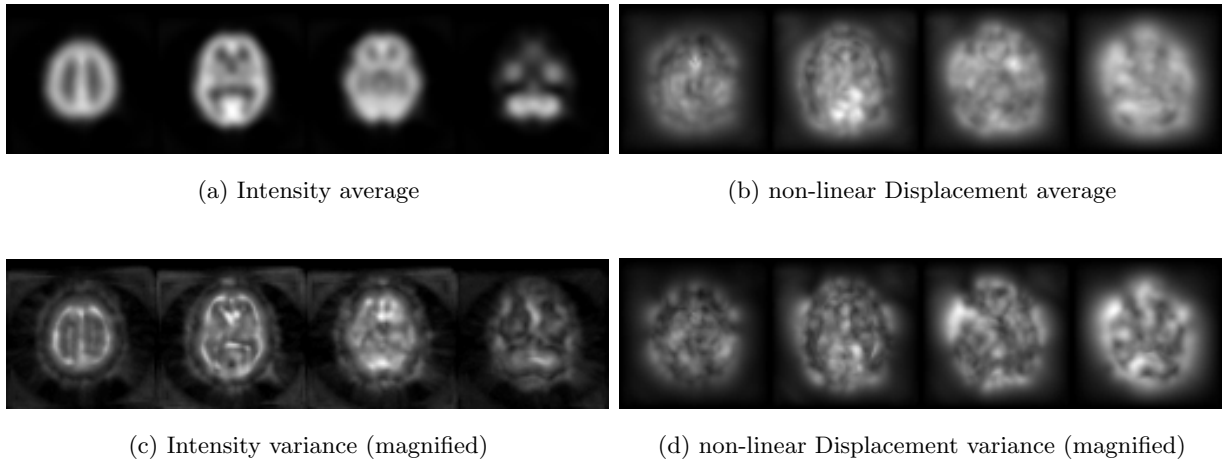
(a) Intensity average

(b) non-linear Displacement average

(c) Intensity variance (magnified)

(d) non-linear Displacement variance (magnified)
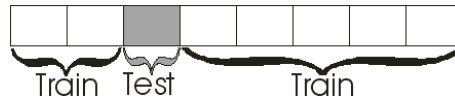
Figure 6. Atlas

Figure 7. Leave-one-out process

visually rCBF studies in nuclear medicine. Moreover such methodology could certainly be applied in several other contexts in SPECT as well as in PET, fMRI and other imaging modalities where an atlas construction is applicable.

Notice that the good success rates obtained in this work must nevertheless be taken with care since the number of SPECT studies is rather limited. This is why we intend to test this approach on a larger number of cases with different and more specific disorders in both SPECT and PET.

ACKNOWLEDGMENTS

REFERENCES

1. R. Holmes, S. Chaplin, K. Royston, and al, "Cerebral uptake and retention of ^{99m}tc-hexamethylpropylene amine oxime (^{99m}tc-hm-pao)," *Nucl. Med. Commun.* **6**, pp. 443–447, 1994.

2. R. Frackowiak, K. Friston, C. Frith, R. Dolan, and J. Mazziotta, *Human Brain Function*, Academic Press, 1997.

3. D. of Cognitive Neurology, "Statistical parametric mapping." *http://www.fil.ion.ucl.ac.uk/spm.*

4. A. Guimond, J. Meunier, and J. Thirion, "Average brain models: A convergence study," *Computer Vision and Image Understanding* **77**, pp. 192–210, February 1999.

5. B. Horn and B. Schunck, "Determining optical flow," *Artificial Intelligence* **17**, pp. 185–204, 1981.

6. D. Barber, "Registration of low resolution medical images," *Phys. Med. Biol.* , pp. 1485–1498, 1992.

7. D. Barber, W. Tindale, E. Hunt, and H. Sagar, "Automatic registration of spect images as an alternative to immobilization in neuroactivation studies," in *Physics in Medecine and Biology*, **40**, pp. 449–463, 1995.

8. M. Mignotte, M. Meunier, J. Soucy, and C. Janicki, "Comparison of deconvolution techniques using a distribution mixture parameter estimation: application in spect imagery," *Journal of Electronic Imaging* **11**(1), pp. 11–25, 2002.

9. M. Mignotte and M. Meunier, "Three-dimensional blinf deconvolution of spect images," *IEEE Trans. on Biomedical* **47**(2), pp. 274–281, 2000.

10. A. Evans and al., "Warping of a computerized 3-d atlas to match brain image volumes for quantitative neuroanatomical and functional analysis," *SPIE Medical Imaging* **1445**, pp. 236–246, 1991.

11. S. Strother and al., "Quantitative comparisons of image registration technique based on high-resolution mri of the brain," *J. Comput. Assist. Tomogr.* **18**(6), pp. 954–962, 1994.